

# Simulation of re-entrant wave dynamics in a 2-D sheet of human ventricle with KCNJ2-linked variant 3 short QT syndrome

Kuanquan Wang<sup>1</sup>, Cunjin Luo<sup>1</sup>, Yongfeng Yuan<sup>1</sup>, Weigang Lu<sup>2</sup>, Henggui Zhang<sup>1,3</sup>

<sup>1</sup>School of Computer Science and Technology, Harbin Institute of Technology, Harbin, Heilongjiang, China

<sup>2</sup>Department of Educational Technology, Ocean University of China, Qingdao, Shandong, China

<sup>3</sup>School of Physics and Astronomy, the University of Manchester, Manchester, UK

## Abstract

Recent studies suggested that short QT syndrome is liable to cause malignant ventricular arrhythmia possibly due to high-frequency re-entrant waves. Our goal was to study the dynamical behaviours of rotors associated with a KCNJ2-linked variant 3 short QT syndrome. A two-dimensional sheet model of human ventricular tissue was implemented to create a short QT syndrome substrate. Electrical action potential of each node was simulated by the ten Tusscher et al. model, which was modified to incorporate changes of  $I_{K1}$  based on experimentally observed data of Kir2.1 function, including WT, WT-D172N and D172N scenarios. Using the model, the minimal length of the S2 stimulus which provided a sufficient substrate for maintaining rotors was computed. It was shown that WT-D172N and D172N mutant  $I_{K1}$  led to abbreviated APD and ERP, resulting in a reduced minimal length of the S2 stimulus to sustain re-entry. This suggested that with the SQT3 Kir2.1 mutation, reentry can be more easily initiated and sustained as compared to the WT condition. This study provides novel insights into the ionic bases of an increased incidence of ventricular fibrillation associated with short QT syndrome, which may cause sudden cardiac death.

## 1. Introduction

Short QT Syndrome (SQT) is associated with increased risks of malignant ventricular arrhythmias leading to sudden cardiac death, possibly due to high-frequency re-entrant waves (rotors). In this study we investigate the arrhythmogenesis of KCNJ2-linked short QT syndrome (SQT3) due to Kir2.1 D172N mutation. SQT3 is identified as a genetic mutation, in which aspartic acid is replaced by asparagines at position 172 in the Kir2.1 potassium channel ( $I_{K1}$  channel) [2]. In their study, El Harchi et al. [3] have shown the Kir2.1 D172N mutation resulted in preferential augmentation of the outward current based on data from whole-cell patch-clamp recordings of Kir2.1 current at ambient and physiological temperatures. In theory, an increased  $I_{K1}$  through mutant Kir2.1 channels would facilitate the initiation

and maintenance of re-entrant waves [4], but the casual link between the two has not been fully established.

In cardiac tissue, re-entrant excitation waves may arise from the instability of electrical wave propagation [5], which are critically correlated with arrhythmic activities of the heart leading to sudden cardiac death [6]. Many computational studies have examined the mechanism of re-entrant wave genesis and the underlying cellular phenomena [7,8]. Fenton et al. provided multiple mechanisms for re-entrant wave breakup [9]. Using a realistic ventricular geometry, Berenfeld and Jalife investigated the effects of interaction between ventricular tissue and Purkinje fibers on re-entrant wave dynamics [10]. Using a computational model of human ventricular tissue, ten Tusscher et al. examined the restitution hypothesis in arrhythmogenesis [11]. Despite these computational studies on arrhythmia, the effect of short QT syndrome on re-entrant wave dynamics has not been analyzed thoroughly. In this study, we investigated the initiation and maintenance of re-entrant waves in ventricular tissue under the short QT syndrome by using a computational method.

Here, following our previous work [1,4], we further investigated the mechanisms by which the Kir2.1 D172N mutation facilitates ventricular reentrant excitation by using 2D idealized computer model of ventricular tissue that took into account of the electrical heterogeneity of transmural ventricle wall. Using this tissue model, we simulated the effects of the Kir2.1 D172N mutation on the re-entrant waves in WT, WT-D172N, D172N conditions. The obtained results provided insights towards understanding the mechanisms by which the Kir2.1 D172N mutation abbreviated ventricular action potential duration that perpetuates reentry.

## 2. Materials and methods

### • Governing equation of electric wave propagation in 2D cardiac tissue.

We adopted the human ventricular cell model developed by ten Tusscher et al. [11] (TP2006 model) in 2D tissue modeling. A schematic of the TP2006

model is shown in Fig. 1, including the ion channels, ion pumps across the cell membrane, and intracellular calcium dynamics. The wave propagation in cardiac tissue was computed using the mono-domain model.

The 2D model of human ventricular tissue represents a tissue sheet across the transmural ventricular wall. The model consisted of 500 cells in length and 300 cells in width. The tissue model was further segmented into an endocardial region, mid-myocardial layer and an epicardial region with a proportion of cells of 25%, 35% and 40%, respectively. These proportions are the same as used in previous studies [1,4,12]. In the presentation of simulation results in visualisation, membrane potential is color represented with blue denoting -90 mV and red denoting +30 mV.

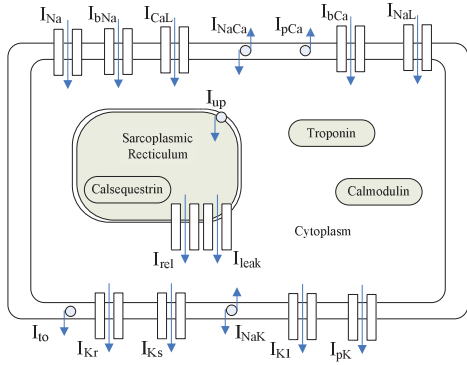


Fig.1. A schematic of human ventricular cell model adopted from ten Tusscher et al. [11].

The governing equation of the 2D cardiac tissue model can be described by the following partial differential equation in reaction-diffusion form:

$$\frac{\partial V_m}{\partial t} = -\frac{I_{ion} + I_{stim}}{C_m} + \nabla \cdot (D \nabla V) \quad (1)$$

where  $V_m$  is transmembrane potential,  $C_m$  is the membrane capacitance,  $I_{stim}$  is the externally applied stimulus current, and  $D$  is the diffusion tensor,  $\nabla$  is the gradient operator,  $t$  is time,  $I_{ion}$  is the sum of ionic currents as described in the following equation:

$$I_{ion} = I_{Kr} + I_{Ks} + I_{K1} + I_{to} + I_{Na} + I_{bNa} + I_{CaL} + I_{bCa} + I_{NaK} + I_{NaCa} + I_{pCa} + I_{pK} \quad (2)$$

A more detailed explanation of the ion currents is given in Ref.[11]. The modified ventricular cell model was then incorporated into the cardiac tissue model of Equation (1).

In order to simulate the functional effects of SQT3, we took into account of three main situations: wide type (WT), heterozygous (WT-D172N) and homozygous (D172N). According to Ref. [4],  $I_{k1}$

formulations were modified based on the experimentally determined properties of Kir2.1 D172N channels, which are described as follows:

$$I_{k1} = G_{k1} \sqrt{\frac{K_o}{5.4}} x_{k1\infty} (V - E_k) \quad (10)$$

$$x_{k1\infty} = \frac{\alpha_{k1}}{\alpha_{k1} + \beta_{k1}} \quad (11)$$

WT:

$$\alpha_{k1} = \frac{0.07}{1 + e^{0.017(V-E_k-200.2)}} \quad (12)$$

$$\beta_{k1} = \frac{3e^{0.0003(V-E_k+100.2)} + e^{0.08(V-E_k-8.7)}}{1 + e^{-0.024(V-E_k)}} \quad (13)$$

$$G_{k1} = 4.8 \text{ ns} / \text{ pF} \quad (14)$$

WT-D172N:

$$\alpha_{k1} = \frac{0.1}{1 + e^{0.023(V-E_k-199.9)}} \quad (15)$$

$$\beta_{k1} = \frac{3e^{0.0002(V-E_k+100.4)} + e^{0.07(V-E_k-9.8)}}{1 + e^{-0.02(V-E_k)}} \quad (16)$$

$$G_{k1} = 6.27 \text{ ns} / \text{ pF} \quad (17)$$

D172N:

$$\alpha_{k1} = \frac{0.1}{1 + e^{0.05(V-E_k-199.9)}} \quad (18)$$

$$\beta_{k1} = \frac{3e^{0.0002(V-E_k+100.1)} + e^{0.08(V-E_k-10.3)}}{1 + e^{-0.006(V-E_k)}} \quad (19)$$

$$G_{k1} = 11.32 \text{ ns} / \text{ pF} \quad (20)$$

$G_{kl}$  is the maximal channel conductance of  $I_{kl}$ ,  $x_{kl\infty}$  is the time-independent inward rectification factor,  $K_o$  is the extracellular potassium concentration.

A forward Euler method was used for the temporal discretization of equation (1), and discrete element method was applied for spatial discretization. A time step of  $\Delta t=0.002$  ms and a space step of  $\Delta x=\Delta y=0.2$  mm were used. The tissue measured  $10 \times 6$  cm<sup>2</sup> in the  $x$  and  $y$  directions, respectively. As we assume an isotropic 2D tissue computation, the diffusion coefficient  $D$  is set to be 0.1. At the beginning, we applied one S1 stimulus, then, the sixth cycle would be applied S2 stimulus at certain time for WT, WT-D172N and D172N conditions.

#### • Initiation of a re-entrant wave

A schematic of the S1-S2 protocol in the 2D tissue model is shown in Fig. 2. We used the S1-S2 protocol to induce a re-entrant wave in the tissue. Initially, the cells located at the boundary surface of  $x=0$  cm were stimulated, and the depolarization wave traveled in the  $x$  direction (S1). After the repolarization wave passed through the boundary surface at  $x=0$  cm, half of the depolarized domain was stimulated to induce instability (S2). In this simulation, Rotors were initiated by the standard S1-S2 stimulation protocol, with a coupling time

interval of 410 ms, 380 ms and 360 ms for the WT, WT-D172N and D172N condition respectively (the stimulation duration of the S2 was 3 ms.)

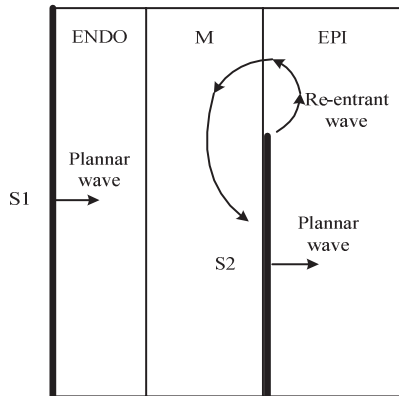


Fig. 2. Schematic of a 2D idealized tissue model with a description of wave propagation and the S1-S2 protocol for including spiral waves.

### 3. Results

The 2D ideal human ventricular tissue model simulated electrical wave conduction under WT, WT-D172N and D172N conductions. Fig. 3 Shows

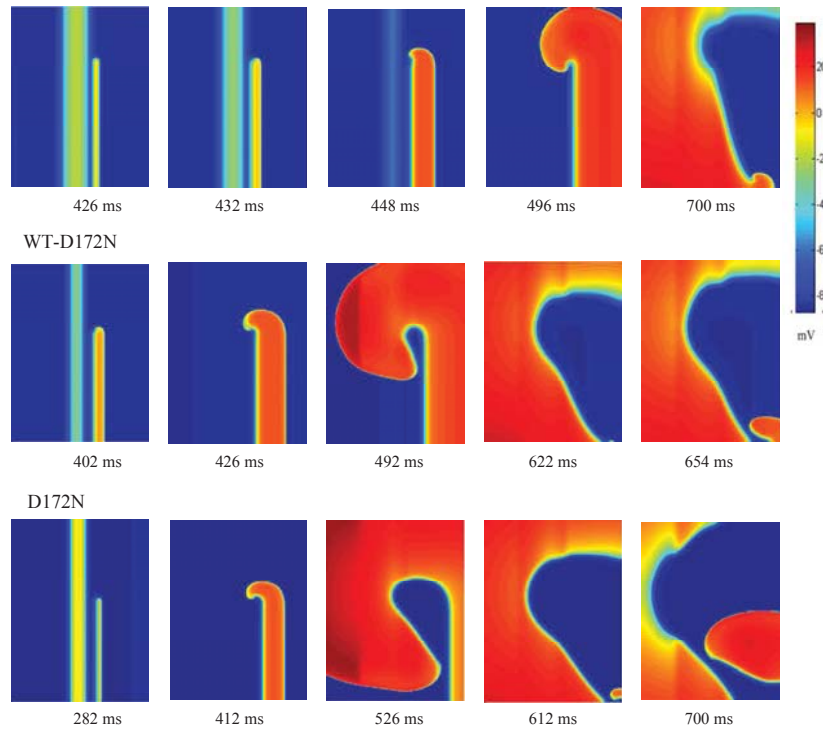


Fig. 3. Sequential contours of action potential propagation for a re-entrant wave under WT, WT-D172N and D172N conditions.

the sequential contours of action potential propagation for a re-entrant wave in WT condition. Then we computed the minimal length of the S2 stimulus which provided a sufficient substrate for maintaining rotors. According to our previous work [1,4], WT-D172N and D172N mutant  $I_{K1}$  led to abbreviated APD and ERP, resulting in a reduced minimal length of the S2 stimulus to sustain re-entry. The computed minimal S2 length was  $\sim 7.16$  cm,  $\sim 6.28$  cm  $\sim 5.84$  cm for WT, WT-D172N and D172N respectively. In addition, the mutation produces an increased gradient of membrane potential across the ventricular tissue, leading to re-entrant waves breaking up under the mutation conditions, implicating a transition from ventricular tachycardia to ventricular fibrillation, due to an increased functional heterogeneity of electrical properties of the tissue.

Our simulation results indicate that under Kir2.1 D172N mutation condition, initiating and sustaining re-entry needs a smaller minimal length of the S2 stimulus. Furthermore, the mutation induces functional electrical heterogeneity that causes re-entrant waves break up, as is shown in Fig. 4. These results demonstrated that the Kir2.1 D172N mutation produces more easily re-entrant waves and affects ventricular tissue's excitability, which may be pro-arrhythmic.

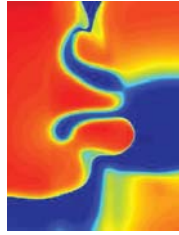


Fig. 4. Re-entrant excitation wave breaks up forming multiple reentrant wavelets under the D172N condition.

#### 4. Discussion

In this study, we delineated the effect of the short QT syndrome on re-entrant wave dynamics by using a computational model that consisted of an electrophysiological model of 2D ventricular tissue based on an existing cellular model and the monodomain method implemented in a 2D discrete element method. In simulations, it was shown that the minimal substrate for initiation and maintenance of reentry is marked smaller in the SQT condition than in the WT condition. In addition, in the WT condition, re-entrant excitation wave presented as a single, more stationary and regular wave, but it breakup forming multiple reentrant wavelets resembling ventricular fibrillation in the SQT condition.

In conclusion, in this study, we characterized the functional impacts of up-regulation of  $I_{K1}$  due to SQT 3 mutation. Our findings of that a D172N mutation resulted in a reduced minimal size of tissue's substrates for initiation and maintenance of reentry, and in the SQT 3 tissue, a marked increase in tissue's functional heterogeneity favoring the formation of multiple reentrant wavelets provide further *in silico* evidence for the proarrhythmic effects of short QT syndrome.

#### Acknowledgements

This study was supported in part by the National Natural Science Foundation of China (NSFC) under Grant No. 61179009, No. 61173086 and No. 61001167.

#### References

- [1] Wang K, Luo C, Wang W, Zhang H, Yuan Y. Simulation of KCNJ2-linked short QT syndrome in human ventricular tissue. *Computing in cardiology* 2013; 40: 349-352.
- [2] Priori, SG, Pandit SV, Rivolta I, Berenfeld O, Ronchetti E, Dhamoon A, Napolitano C, Anumonwo J, Di Barletta MR, Gudappakkam S, Bosi G, Stramba-Badiale M & Jalife J.A novel

form of short QT syndrome (SQT3) is caused by a mutation in the KCNJ2 gene. *Circ Res* 2005; 96: 800-7.

[3] EL Harchi A, Mcpate MJ, Zhang Y, Zhang H & Hancox JC. Action potential clamp and chloroquine sensitivity of mutant Kir2.1 channels responsible for variant 3 short QT syndrome. *J Mol Cell Cardiol* 2009; 47: 743-7.

[4] Adeniran I, EL Harchi A, Hancox JC & Zhang H. Proarrhythmia in KCNJ2-linked short QT syndrome: insights from modelling. *Cardiovasc Res* 2012; 94: 66-76.

[5] D'Almoncourt CN, Zierhut W & Bluderitz B. "Torsade de pointes" tachycardia. Re-entry or focal activity? *Br Heart J* 1982; 48: 213-6.

[6] Rodriguez LM, Sternick EB, Smeets JL, Timmermans C, Den Dulk K, Oreto G & Wellens HJ. Induction of ventricular fibrillation predicts sudden death in patients treated with amiodarone because of ventricular tachyarrhythmias after a myocardial infarction. *Heart* 1996; 75: 23-8.

[7] Gima K & Rudy Y. Ionic current basis of electrocardiographic waveforms: a model study. *Circ Res* 2002; 90: 889-96.

[8] Rudy Y. From genome to physiome: Integrative models of cardiac excitation. *Annals of Biomedical Engineering* 2000; 28: 945-950.

[9] Fenton FH, Cherry EM, Hastings HM & Evans SJ. Multiple mechanisms of spiral wave breakup in a model of cardiac electrical activity. *Chaos* 2002; 12: 852-892.

[10] Berenfeld O & Jalife J. Purkinje-muscle reentry as a mechanism of polymorphic ventricular arrhythmias in a 3-dimensional model of the ventricles. *Circ Res* 1998 82, 1063-1077.

[11] Ten Tusscher KH & Panfilov AV. Alternans and spiral breakup in a human ventricular tissue model. *Am J Physiol Heart Circ Physiol* 2006; 291: H1088-100.

[12] Zhang H & Hancox JC. In silico study of action potential and QT interval shortening due to loss of inactivation of the cardiac rapid delayed rectifier potassium current. *Biochem Biophys Res Commun* 2004; 322: 693-9.

Address for correspondence.

Kuanquan Wang  
Mailbox 332, Harbin Institute of Technology  
Harbin 150001, China  
wangkq@hit.edu.cn